

# Determining the optimal dimensions of the pillars under static and dynamic loads in room and pillar mines (Case study: Tabas central coal mine)

M. Heidarnajad<sup>1</sup>, A. Azhari<sup>1\*</sup>, M. Ahour<sup>2</sup>, E. Ghasemi<sup>1</sup>

1- Dept. of Mining Engineering, Isfahan University of Technology, Isfahan, Iran

2- Dept. of Civil Engineering, Yazd University, Yazd, Iran

\* Corresponding Author: [aazhari@iut.ac.ir](mailto:aazhari@iut.ac.ir)

(Received: October 2021, Accepted: February 2022)

## Keywords

Static analysis  
Dynamic analysis  
Room and pillar  
Numerical modeling  
Optimal pillar width

## Abstract

A pillar dimension in room and pillar mining method has been always a technical and economical issue for mining and rock mechanic engineers. The strength of the pillars is usually determined by empirical relationships, which have been determined by experience and the data collected from the coal mines of the United States, South Africa, and China, and which, except in one case, have never been considered seismic loads. This study aims to define the optimum pillar dimension based on the pillar strength derived from a new approach implemented in the numerical modeling by gradually applying an increasing load on the pillar and monitoring its displacement, using the Central section of Tabas coal mine data. The results are compared with the method of Salamon-Munro (1967) which is one of the most commonly used empirical methods. This comparison shows that the strength obtained from the numerical method for pillar widths of less than 15 m is well consistent with the empirical Salamon-Monroe method, whereas the difference between the results of the two methods increases progressively with a pillar width increment. The safety factor of the pillar is then defined by dividing the obtained pillar strength and monitoring critical stresses, under static and dynamic conditions. Tabas (1978) earthquake with 7.4 magnitudes is used for dynamic analyses. The results show that the optimal width of the pillar in the static and dynamic states is 12 and 15 meters, respectively. Moreover, curve fitting with high regression to the results obtained in both static and dynamic states, relations in terms of width to height ratio are presented for use in other areas of the mine with similar geomechanical conditions.

## 1. INTRODUCTION

The room and pillar method is a self-stabilizing method in which the mineral is exploited in the form of chambers. In this mining method, a part of the deposit remains to support the roof, which in some cases cannot be recovered. The integrity of a coal mine mainly depends on the pillars and their design, therefore the design of these foundations is particularly sensitive [1]. In underground mining, the geomechanical conditions of the area rarely allow the extraction of 100% of the mineral, and some of the deposit is left. The remaining pillars are the elements that support and control the created space; therefore, some of the deposits will not be recoverable. The ratio between the

mined deposit and the whole deposit is called the recovery coefficient [2]. Pillar design is one of the most important and complex issues in the field of stability and land control in underground mines, especially room and pillar mines, which has been mostly studied in coal-producing countries. The knowledge of pillar design in the United States dates back to almost a hundred years ago when the reverse analysis was developed. For instance, in 1980, based on statistical studies conducted in the United States, the traditional method of designing the pillars was introduced, which includes three steps, namely, estimating the load on the pillars using the tributary area theory; computing the pillar strength using the experimental relationships of the pillar; and calculating the safety factor [3].

In 1981, Bieniawski introduced a step-by-step method for measuring the dimensions of coal pillars in the room and pillar coal mines. In this approach, the load was also calculated similarly to the traditional method using the tributary area theory [3]. In 1970, Salamon proposed an experimental relationship based on the ratio of width to height of the pillars, which is obtained for a wide range of African coal mines. Galvin et al. (1999) conducted a field study based on the collected data from Australian coal mines as well as data obtained by Salamon (1970) [4-9]. Wang (2011) and Jiang et al. (2012) also conducted research on these mines [10]. Dabbagh et al. (2009) investigated the extent of subsidence and the corresponding strains by mining inclined coal seams using displacement discontinuity and finite difference approach [11]. In 2014, Xu et al. analyzed the stability of coal pillars in inclined layers that are left behind to prevent water intrusion into the mining area using analytical and numerical methods [12]. Their studies have shown that the proposed experimental method for the pillar design is in good agreement with numerical methods. Jun De et al. (2014) numerically modeled the remaining optimal pillar dimensions in the 17 degrees layers. The results on pillars with a width of 3 to 10 meters have shown that by increasing the width of the pillars, the probability of pillar failure decreases and pillar failure in pillars with a width of 3 meters would be more than in other pillars. The results of this research have shown that a pillar with a width of 5 meters is an optimized design [13]. Najafi et al., (2016) numerically investigated the effect of coal seam slope and pillar width variance on the stress distribution of pillars. The results showed that with increasing seam dip and pillar width the normal stress increases, whereas the shear stress component decreases. They suggested larger pillar widths for steeper coal seams [14]. Dehghan et al. (2012) conducted a study examining the stress distribution in pillars of a stope and pillar mine in different depths considering the mining sequence, using numerical analysis. The results show that as long as the pillars are in the elastic state the empirical results are in good agreement with the ones from the numerical approach. However, in the plastic state of pillars, there is a significant difference between empirical and numerical results [15]. The effects of the earthquake during the life of the mine and even after it should not be ignored. For instance, on March 11, 2011, a magnitude 9.0 earthquake struck most parts of Japan, including Miyagi and Iwata, in which there are many abandoned coal mines. These mines are generally located in urban areas and the remained pillars of these mines have

been failed by the earthquake, which led to the formation of cavities in the urban area. Aydan and Kawamoto (2004) showed that these mines posed a serious threat to urban infrastructure, causing failure and subsidence on the surface [16]. Dan et al. (2006) built a physical model of an abandoned room and pillar mine using a piled rock mass on a vibrating table. They found that for shallow room and pillar mines, surface failures and sinkholes appear much faster on the ground compared to deep mines. Nishida et al. (1984), and Walton and Cobb (1984), concluded that the stress applied to the pillars increased with increment depth and the stress in the roof layers was greater at shallower depths [17]. Nishida et al. In 1984, as well as Walton and Cobb in 1984, believed that the stress applied to the pillars increases with increasing depth, whereas the stress in the roof layers is greater at shallower depths. By constructing this physical model, Aydan found that in shallow mines, roof collapse is the main reason for failure and surface subsidence while pillar failure is the reason for ground subsidence in deep room and pillar mines [17]. Aydan et al. (2006) performed a physical model of an abandoned room and pillar mine using a piled rock mass on a vibrating table. Sinkhole settlements appear much faster on the ground [18]. Based on these observations and studies conducted on the seismic stability of room and pillar mines, Aydan (2010) presented a pseudo-static relation based on the failures observed in the abandoned mining area of Yamoto city, Japan, due to the 2003 Miyaji Hokubo earthquake. According to this study, he proposed quasi-static relations defining a seismic coefficient to apply seismic load to the room and pillar mine. For this, the stress on the pillars is calculated as follows [18].

$$\sigma_p = \rho g H \frac{A_t}{A_p} \left[ 1 + 6\alpha \frac{H}{W} \cdot \frac{y}{W} \right] \quad (1)$$

where  $\rho$  is the overburden density,  $g$  is the gravity acceleration,  $H$  is the overburden height,  $A_t$  is the tributary area,  $A_p$  is the loaded pillar area,  $W$  is the pillar width,  $y$  is the distance from the center of the pillar, and  $\alpha$  is the seismic coefficient of the region calculated from Eq. 3. It should be noted that if the maximum tensile and compressive strength occurs on both sides of the pillar and the tensile strength between the pillar and the roof is considered zero, the maximum compressive stress in the pillar would be calculated as [18]:

$$\sigma_p = \sigma_{PO} \frac{1}{(1 - \epsilon)^2} \left[ 1 + \frac{6}{(1 - \epsilon)} \left( \alpha \frac{H}{2W} \epsilon \right) \right] \quad (2)$$

$$\alpha = \frac{W}{3H} [5\epsilon + 1]$$

where,  $\sigma_{p0}$  is equal to  $\rho g H \frac{A_t}{A_p}$  and  $\epsilon$  is equal to  $\frac{e}{W}$  and  $e$  is equal to  $w \cdot w^*$  and  $A_p^*$  is equal to  $w^* \cdot w^*$ , and  $w^*$  is the effective pillar width.



Figure 1. Physical model of a shallow (left) and deep (right) room and pillar mine subjected to the seismic load [5,9]

Physical model tests simulating the abandoned room and pillar mines using a vibrating table showed that the roof layers also failed under bending, where  $\alpha$  can be calculated from the following equation:

$$\alpha = \frac{\sigma_t}{\rho g w \left( \frac{A_t}{A_p} - 1 \right)} - \frac{W}{2H} \left( \frac{A_t}{A_p} - 1 \right) \quad (3)$$

where,  $\sigma_t$  is the tensile strength of the pillar [17]. A summary of the empirical and physical modeling studies is given in Table 1.

Table 1. Summary of the relationships presented by different researchers to estimate the stresses on a pillar under static and dynamic loads

researchers	Research Methods	Pillar Strength Formulas	Type of analysis	Shape of the pillars	Coefficients
Salamon-Munro	Empirical	$K h^\alpha w^\beta$	static	Square	$\alpha = 0.66$ $\beta = 0.46$
Bieniawski	Empirical	$S_1 = 0.64 + 0.36 \left( \frac{W}{h} \right)$	static	Square	-
Madden	Empirical	$K \frac{R_O^b}{V^a} \left\{ \frac{b}{\epsilon} \left[ \left( \frac{R}{R_O} \right)^\epsilon - 1 \right] + l \right\}$	static	Square	$a = 0.0667$ $b = 0.5933$
Mark-Chase	Empirical	$S_1 = \left( 0.64 + 0.54 \left( \frac{W}{h} \right) - 0.18 \left( \frac{W}{h} \right) \right)$	static	Rectangular	-
Aydan et al	Physical model	$\sigma_{p0} \frac{1}{(1-\epsilon)^2} \left[ 1 + \frac{6}{(1-\epsilon)} \left( \alpha \frac{H}{2W} - \epsilon \right) \right]$	Pseudo-static	Square	-

where, K is the constant representing the strength of the coal material (MPa), W is the pillar width (m), h is the pillar height, S<sub>1</sub> is the critical strength of the coal (MPa), R is the pillar width to height ratio, R<sub>O</sub> is the critical width to height ratio of the pillar, V is the pillar volume (m<sup>3</sup>),  $\epsilon$  is the strength increase rate, L is the pillar length (m). As presented limited studies have been conducted on the seismic stability of room and pillar mines where a few formulations have been expressed for predicting safety factors in the studied areas. This study aims to determine the optimum width of the pillar in the room and pillar mines, according to the allowable safety coefficient, using numerical modeling under static and dynamic conditions. For this purpose, the geomechanical data of Tabas Central Mine, with a room and pillar mining method, where the 7.4 magnitude Tabas earthquake (1978) is used for the dynamic analyses.

## 2. CASE STUDY

The study area in this research is the central part of Tabas Coal Mine, which is located 85 km south of the Tabas, South Khorasan province. Figure 2 maps the central room and pillar part of Tabas mine. In this mine, C1 coal layer has been extracted from the room and pillar method. This layer is about 2 meters thick and has a slope of 8-12 degrees. The immediate roof of this mine is weak and includes mud with a thickness of 0.1 to 0.2 m and siltstone/sandstone with a thickness of 3 m where the lithology of the area up to the ground level is mainly siltstone. Also on the floor, there is mudstone with a thickness of 1 to 1.3 meters with sandstone underneath. Figure 3 shows the thickness and material of the geological layers in this area. The compressive strength of the coal is estimated to be about 6 MPa from the uniaxial compressive test [3]. The proposed

design of the central mine consists of two access tunnels, the main panel, and the east and west panels on both sides of the main panel. The main

panel is considered in this study, the geotechnical characteristics of which are presented in Table 2.

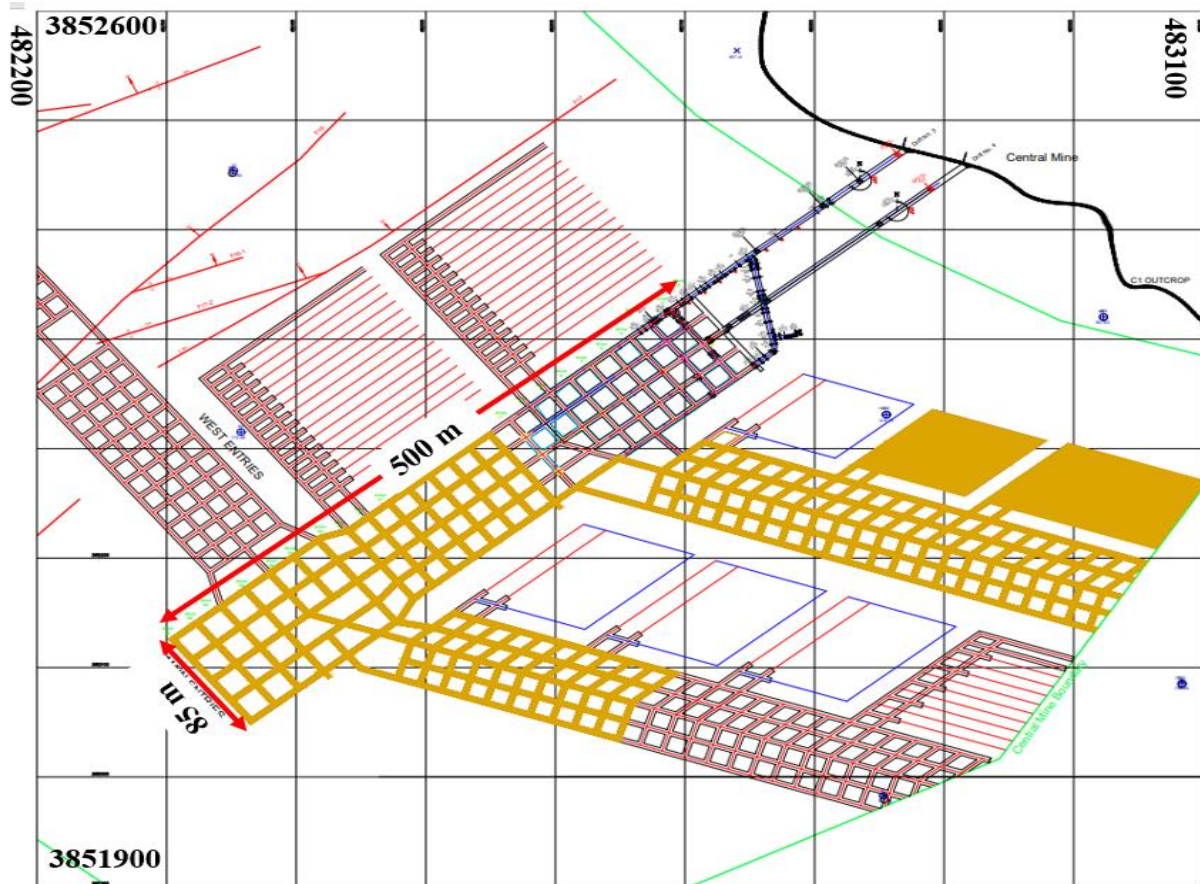


Figure 2. Plan view of the Tabas Central Coal Mine [19]

Table 2. Geomechanical characteristics used in numerical modeling [19]

Parameter	Unit	Sandstone	Siltstone	Coal
Cohesion	MPa	8.69	1.3	0.6
Internal Friction angle	degree	21.75	24.12	15 - 25
Unit weight	kN/m <sup>3</sup>	27	27.2	16
Shear modulus	GPa	1/42	0.895	1.26
Bulk modulus	GPa	1.365	1.492	2.11

### 3. DETERMINING THE OPTIMAL PILLAR WIDTH UNDER STATIC CONDITION

As mentioned the purpose of modeling in this research is to first find the optimal pillar width in the pre-seismic and post-seismic states. Prior to dynamic analysis, the static stability of pillars should be investigated. The height of the coal seam is considered 2 meters with a shallow dip of a

maximum of 12 degrees, which results in a mean depth of 80 meters for the pillars. Figure 4 shows the geometry of the constructed model along with the boundary conditions in the static state. The boundaries of the overburden and the layers underneath the coal seam are fixed in the horizontal directions while the boundaries of the coal seam are considered free boundaries to expand under the applied normal stress. As can be seen in Figure 4, in order to speed up the numerical solution process, the part of the overburden (60 meters) whose deformation has a negligible effect on the pillar stress changes has been replaced as an equivalent load of 1.6 MPa. In order to investigate the pillar behavior, the elastoplastic Mohr-Columb behavioral criterion is implemented. The geomechanical parameters are presented in Table 2.

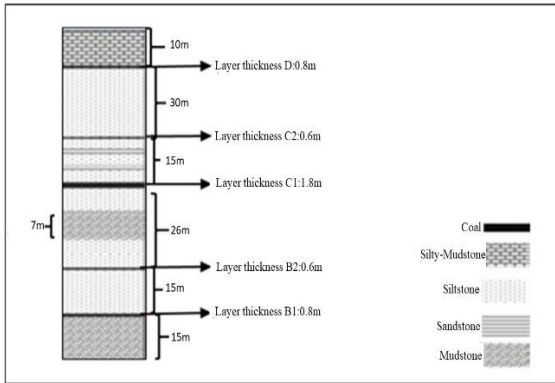


Figure 3. Stratigraphic column of the central zone of Prodeh Tabas [19]

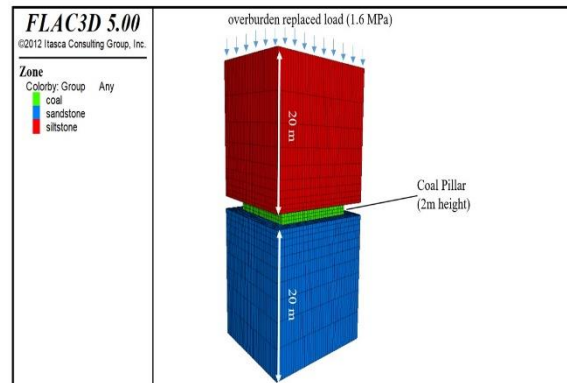


Figure 4. Static boundary conditions

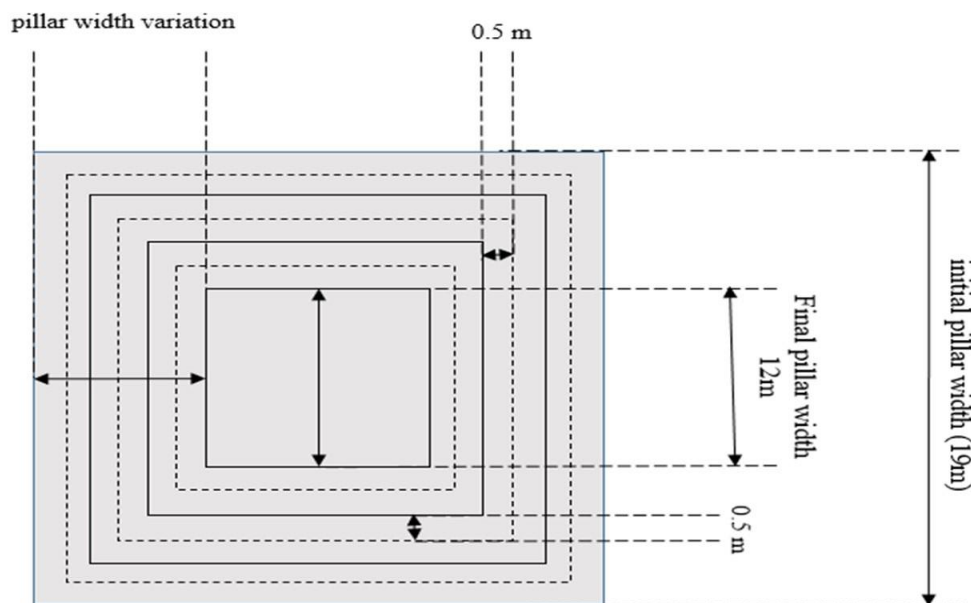


Figure 5. Plan view of the pillar section in each excavating stage

In order to find the optimal width of the pillar, 0.5 meters of the width of the pillar in each direction are excavated in each stage and the safety factor is obtained accordingly. Figure 5 shows the plan view of the pillar sections after each stage. To obtain the safety factor, the pillar strength is first estimated using a FISH scripting language, where a slight speed is applied to the top of the pillar causing a slight displacement. The resistance of the pillar against the displacement is monitored and defined as the pillar strength. As an example, Figure 6 shows the curve of applied stress versus solving for a 12 m pillar width. As can be seen, the stress is increased first and then keeps constant at 9MPa which indicates the yield of the pillar to this amount of stress, which is considered the pillar strength. A similar process has been performed to find the pillar strength with different widths in various excavating stages. After obtaining the pillar strength and monitoring the critical stresses by dividing the pillar strength by

the critical stress, the safety factor for different pillar widths is obtained. Figure 7 illustrates the stress distribution contours in vertical (Z) and horizontal (X and Y) directions under static conditions. The results obtained from this method are also compared with the empirical Salomon-Munro relationship presented in Table 1, where K was considered 6.1 MPa,  $\alpha$  and  $\beta$  constants were 0.66 and 0.46, respectively.

The safety factor obtained from these two methods for different excavating stages is presented in Table 3. Normalizing the results of numerical analysis and experimental relationships for the ratio of width to height of pillars with different widths, Figure 8 depicts the comparison of safety factors in both numerical and empirical methods. An error analysis is also performed comparing to the Salomon-Munro (1967) and numerical results, using Eq 4.

**Table 3. Comparison of safety factors derived from numerical and empirical approaches in a static state**

Pillar width	Safety factor Salomon and Munro	Safety factor Numerical method
19	6.46	10.51
18	5.97	8.5
17	5.36	6.76
16	4.68	5.24
15	3.94	4.07
14	3.16	2.99
13	2.37	2.03
12	1.51	1.2

$$Relative\ Error = \left| \frac{SF_N - SF_{S-M}}{SF_{S-M}} \right| \quad (4)$$

where,  $[[SF]]_N$  and  $[[SF]]_{(S-M)}$  are safety factors obtained from the numerical and empirical analyses, respectively. Table 4 presents the error analysis results between the numeral and Salomon-Munro empirical analysis.

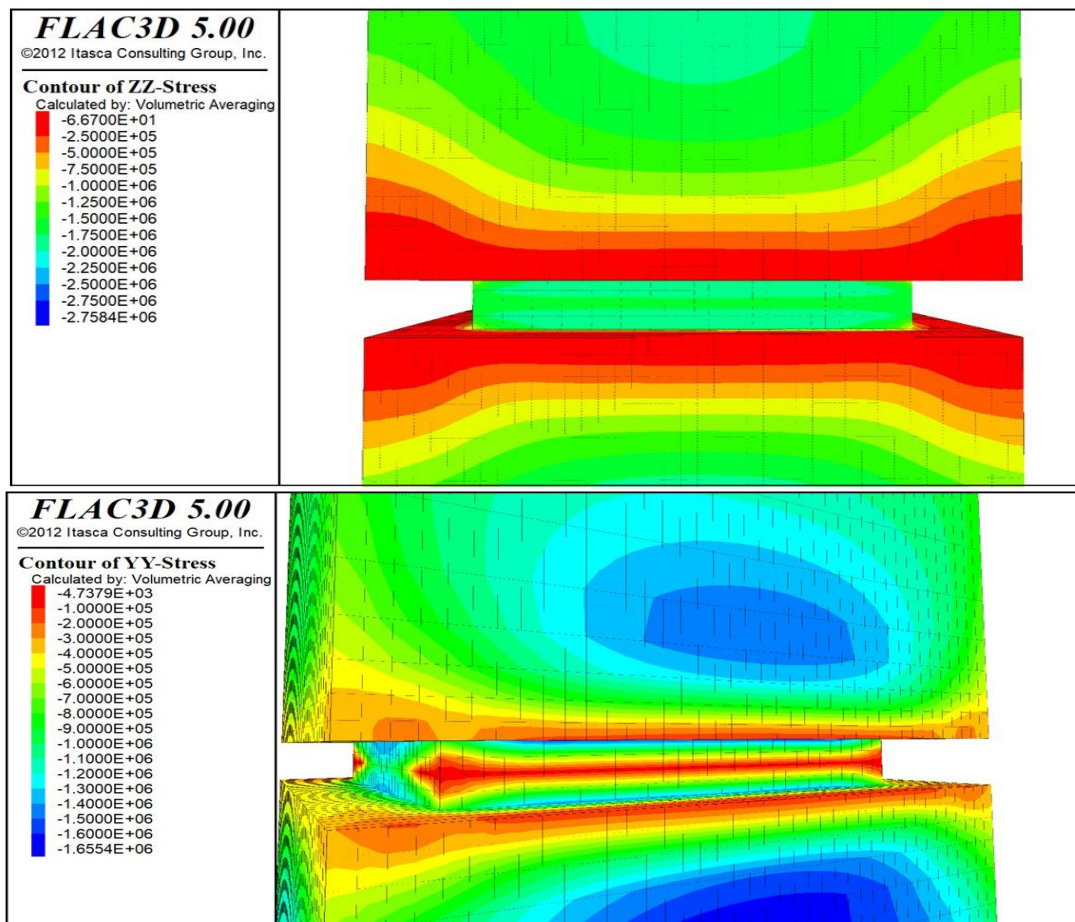


**Figure 6. Stress distribution contours in vertical (top) and horizontal (bottom) directions under static condition**

**Table 4. The error analysis results between the numerical and Salomon-Munro empirical analysis**

W/H	Salomon-Munro	Numerical	Error
9.50	6.46	10.51	0.63
9	5.97	8.5	0.42
8.5	5.36	6.76	0.26
8	4.68	5.24	0.12
7.5	3.94	4.07	0.03
7	3.16	2.99	0.05
6.5	2.37	2.03	0.14
6	1.51	1.2	0.21

Figure 7 and error analysis show that the safety factors obtained from numerical modeling in pillars with widths less than 15 m are in good agreement with the Salamon and Munro (1967) experimental method. While for the width-to-height ratio greater than 7.5 the difference

between the numerical method and the experimental method is increasing progressively, whereas, for the width-to-height ratio of 9.5, this increase reaches 60%.

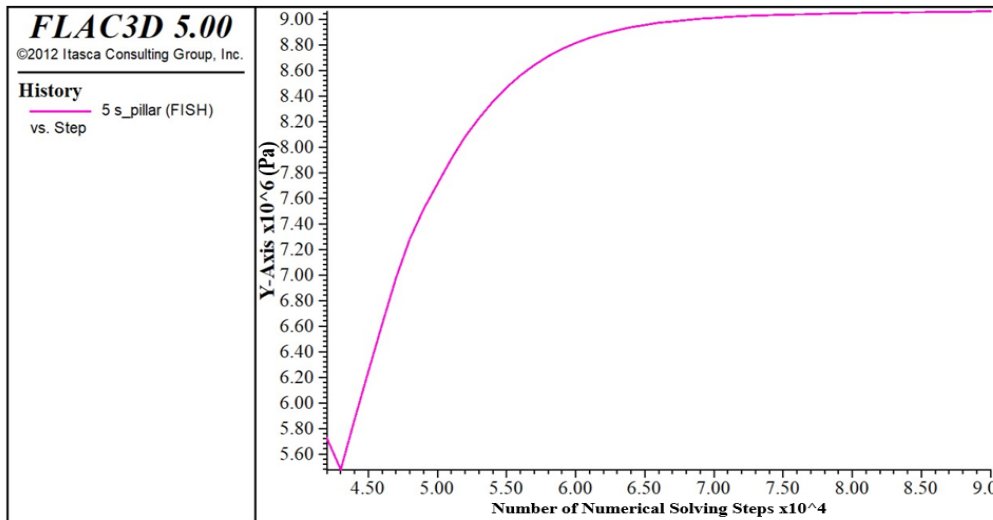


Figure 7. Determining the pillar strength with a width of 12 meters at a depth of 80 meters

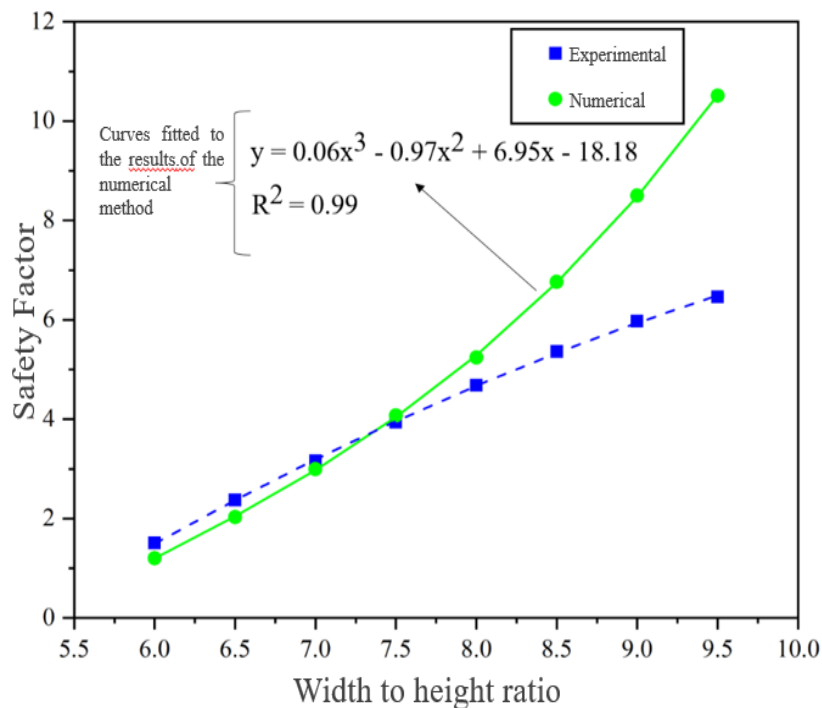


Figure 8. Comparison of safety factors between numerical and empirical approaches in the static state

**4. DETERMINING THE OPTIMAL PILLAR WIDTH UNDER DYNAMIC CONDITIONS**

After investigating the static stability and the effect of pillar width on the static safety factor, the

dynamic safety factor of the pillars is evaluated in different excavating stages. In dynamic analysis, considerations must be taken to ensure the proper wave travels through the model. These considerations include mesh dimensions, boundary conditions, and damping coefficient

[20]. The dimensions of elements in numerical modeling are important in terms of problem-solving time and proper propagation of the seismic wave through the simulation. The large dimensions of the elements may cause the reflection of the wave and consequently the improper passage of the earthquake wave, while the excessive size of the elements significantly increases the speed of problem-solving. Thus, the dimensions of the elements are considered according to Eq. (5) to be a maximum of one-eighth of the wavelength passing through the medium.

$$l_{\max} = \frac{C_s}{8f_{\max}} \quad (5)$$

$$C_s = \sqrt{G/\rho} \quad (6)$$

where  $l_{\max}$  is the maximum dimension of the element,  $C_s$  is the velocity of shear wave propagation in the medium obtained from Eq. 8,  $f_{\max}$  is the highest frequency of an earthquake wave in which the wave has energy.  $G$  and  $\rho$  are the shear modulus and rock mass density, with values of 1.42 GPa and 2700 kg/m<sup>3</sup>, respectively. Therefore, the wave velocity is 725 m/sec, and the maximum mesh dimensions is 18 meters, where the element dimensions have not exceeded this value in the models. Damping is another phenomenon that originates from the reduction of wave energy in propagating through the medium. Based on science experiences, the amount of damping in geotechnical materials is in the range of 2 to 5% of the critical damping. In this dynamic analysis, the Mohr-Columb failure criterion is used with local damping equal to 5% of the critical damping. In addition, the necessity to ensure the proper travel of the wave through the model, and the behavior of the wave reaching the boundaries

must also be guaranteed. The wave is reflected and returned to the model when it encounters the boundary of the static model. Thus the boundary must be defined in a way that mimics the actual condition. For this purpose, in dynamic modeling, the quiet (viscous) boundary is used to absorb the wave and the free field boundary to pass the wave. In this research, free borders are used around the model and a quiet boundary is used at the bottom of the model (Figure 9). To use the viscous boundary in the model floor, the seismic load is applied to the model floor as shear stress. Eq. (7) presents the conversion of wave velocity to equivalent shear stress [20].

$$\sigma_s = -2(\rho C_s)v_s \quad (7)$$

where  $\sigma_s$  is the applied shear stress,  $v_s$  is the velocity of the input shear wave applied at the boundary,  $\rho$  is the density of the medium, and  $C_s$  is the velocity of the shear wave passing through the medium. Based on this, the accelerogram data of the Tabas earthquake in 1978 with a magnitude of 7.4 Richter for 11 seconds have been considered in the simulations. Figure 10 shows the recorded accelerations in three directions of the Tabas earthquake. According to this figure, the peak ground acceleration (PGA) in the horizontal directions (X- and Z-directions) are 9m/s<sup>2</sup>, while the PGA for the vertical direction (Y) is 7m/s<sup>2</sup>. The PGA has mostly occurred between seconds 2 and 3 of the recorded accelerations. The duration of the earthquake is 11 seconds. By integrating acceleration data and making necessary corrections such as baseline, the velocity versus time is calculated, which is performed by SeismoSignal software. Eq. 9 is then utilized to convert the seismic waves to stress and is applied to the model in three directions up to the bottom of the model with a viscous boundary.

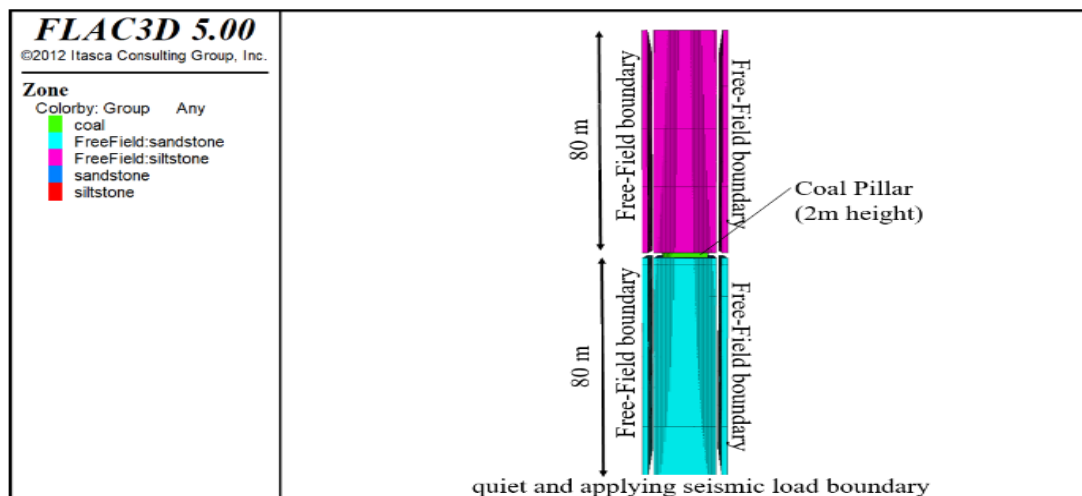


Figure 9. Free and quiet boundary conditions illustration on model sides and bottom of the model

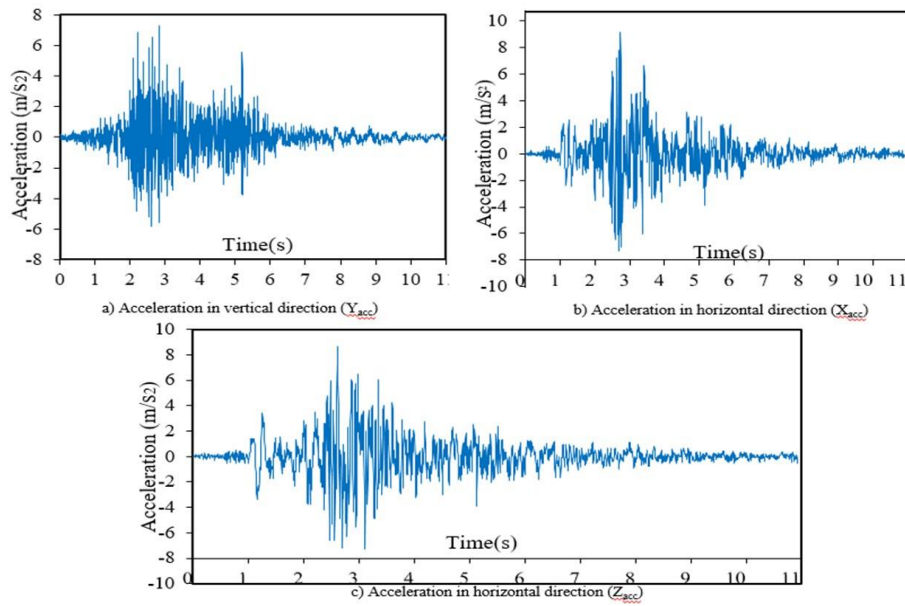


Figure 10. Applied acceleration from Tabas (1978) earthquake, Mw: 7.4, in three directions

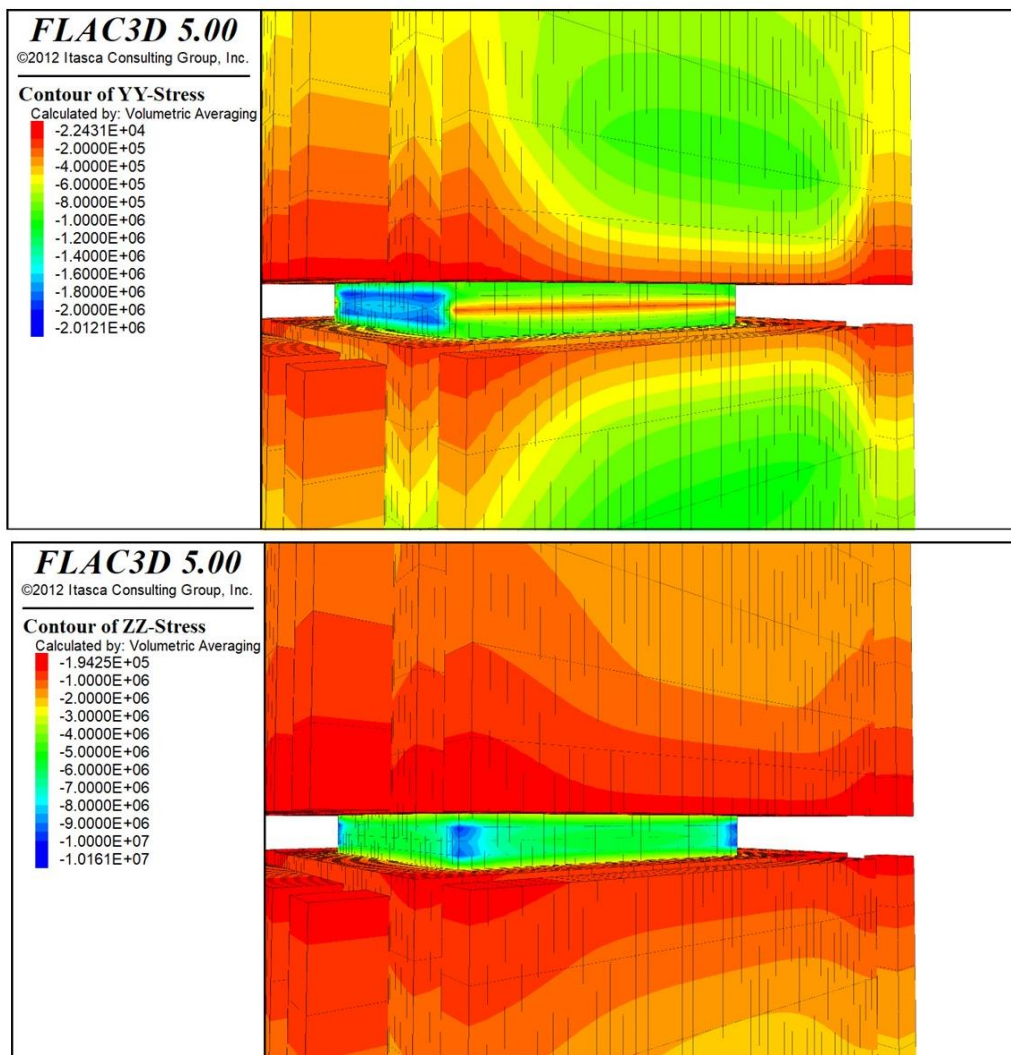
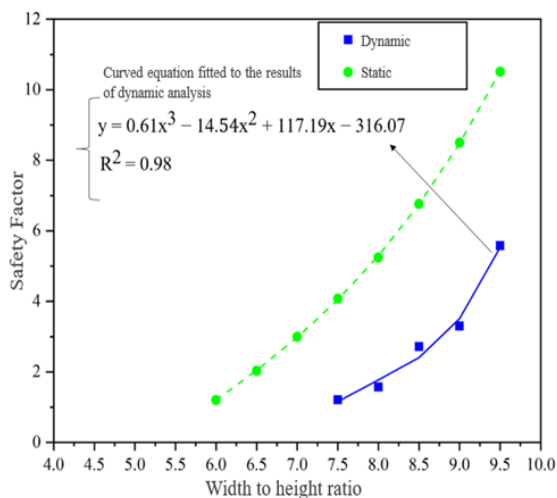


Figure 11. Stress contours of the pillar under dynamic loads.

**Table 5. Obtained safety factors from numerical modeling in static and dynamic modes**

Pillar width (m)	Dynamic Safety factor	Static Safety factor
19	5.58	10.51
18	3.3	8.5
17	2.72	6.76
16	1.57	5.24
15	1.21	4.07
14	unstable	2.99
13	unstable	2.03
12	unstable	1.2

To calculate the dynamic safety factor the stress contours are obtained from numerical simulation under dynamic loads. Figure 11 depicts the stress contours of the pillar under dynamic loads. Then the pillar strength derived from the previous section is divided by the pillar stress to obtain a dynamic safety factor. Table 5 presents the static and dynamic safety factors for various pillar widths and Figure 12 plots the numerical static and dynamic safety factors.

**Fig12. Comparison of safety factors obtained in static and dynamic modes**

According to the curve fitting of the graph derived from numerical dynamic analysis ( $R^2:0.99$ ), Eq. (8) is presented for the safety factor in terms of width to height ratio ( $w/h$ ).

$$SF = C_1 \left(\frac{w}{h}\right)^3 + C_2 \left(\frac{w}{h}\right)^2 + C_3 \left(\frac{w}{h}\right) + C_4 \quad (8)$$

where  $w$  is the pillar width,  $h$  is the pillar height, and  $C_1$ ,  $C_2$ ,  $C_3$ , and  $C_4$  are the constants, defined as 0.6, -14.5, 117.2, and 316, respectively.

## 5. CONCLUSION

Given that the dimensions of the pillars in underground mines have to be determined according to technical and economical considerations, the optimum pillar should be designed considering these two factors. The strength of the pillars is generally determined by empirical relationships, which have been determined by experience and the data collected from the mines of other countries, including the United States, South Africa, and China, and which, except in one case, have never considered seismic loads. In this research, an attempt was made to determine the pillar strength by implementing a new approach to numerical modeling by gradually applying a load on the pillar and monitoring its displacement. Tabas coal mine was considered as the case study implementing the proposed approach. The results showed that under static loads shrinking the pillar width from 19 to 12 meters will significantly reduce the safety factor while it is still in the acceptable range (1.2). However, under the dynamic load of the Tabas earthquake (1978), the minimum pillar width would be 15 meters with a safety factor of 1.21. It was also observed that the decreasing trend of the static and dynamic safety factors due to pillar width shrinkage is almost the same. Moreover, the results were compared with the Salamon-Munroe method which is one of the most widely used empirical methods. This comparison showed that the strength obtained from the numerical method for pillar widths of less than 15 m is well consistent with the experimental.

## REFERENCES

- [1] Jiang, Yaodong, Et Al. "Assessment And Mitigation Of Coal Bump Risk During Extraction Of An Island Longwall Panel". International Journal Of Coal Geology,95: 20-33, 2012.
- [2] Atai, Mohammad, "Underground Mining, Volume 2: Self-Maintenance Methods", Shahroud University of Technology Press, 2005 ) In Persian)
- [3] Ghasemi, E., Shahriar, K., Hashemalhosseini, H. (2012). Development of a new method for coal pillars design in room and pillar mines. Journal of Analytical and Numerical Methods in Mining Engineering, 1(2), 15-23.
- [4] Sheorey PR. "Design Of Coal Pillar Arrays, Chain Pillars". In: Hudson JA, Et Al., Editors.Comprehensive Rock Engineering, Vol. 2. Oxford: Pergamon. P. 631-70, 1993.

- [5] Galvin, Jim M.; Hebblewhite, Bruce K.; Salamon, Miklos Dg. University Of New South Wales, "Coal Pillar Strength Determinations For Australian And South African Mining Conditions". In: Proceedings Of The Second International Workshop On Coal Pillar Mechanics And Design, National Institute For Occupational Safety And Health, Report Ic. P. 63-71, 1999.
- [6] Galvin, Jim, Et Al. "Considerations Associated With The Application Of The Unsw And Other Pillar Design Formulae. In: Golden Rocks", The 41st Us Symposium On Rock Mechanics (Usrms). American Rock Mechanics Association, 2006.
- [7] Wang, Hongwei, Et Al. "Numerical Investigation Of The Dynamic Mechanical State Of A Coal Pillar During Longwall Mining Panel Extraction". Rock Mechanics And Rock Engineering, 46.5: 1211-1221, 2013.
- [8] Bieniawski, Z. T. "The Effect Of Specimen Size On Compressive Strength Of Coal". In: International Journal Of Rock Mechanics And Mining Sciences & Geomechanics Abstracts. Pergamon. P. 325-335, 1968.
- [9] Salamon, M. D. G.; Ozbay, M. U.; Madden, B. J. "Life And Design Of Bord-And-Pillar Workings Affected By Pillar Scaling". Journal Of The Southern African Institute Of Mining And Metallurgy, 98.3: 135-145, 1998.
- [10] Ghasemi, E.; Shahriar, K. "A New Coal Pillars Design Method In Order To Enhance Safety Of The Retreat Mining In Room And Pillar Mines". Safety Science, 50.3: 579-585, 2012. (In Persian).
- [11] Dabagh, A., Fatehi Marji, M., Forghani, H., "Simulation of Subsidence with a Higher Order Displacement Discontinuity Method". International Journal of Mining Engineering, Volume 4, Issue 7, Page 53-6, (2009), (In Persian).
- [12] Xu, B., Yin, S., Zhang, X., & Wu, J. Research on the Stability of Waterproof Coal Pillar in Steep Seam under Aquifers. An Interdisciplinary Response to Mine Water Challenges - Sui, Sun & Wang, China University of Mining and Technology Press, Xuzhou, ISBN 978-7-5646-2437-8, (2014).
- [13] Jun De, Q. I., Jing, C. H. A. I., & Zhang, J. (2014). Numerical Design of Pillar Width in the Inclined Coal Seam. Advanced Materials Research, 977. (2014).
- [14] Najafi, M., & Motahhari, M., & Norouzi, M. (2016). Numerical Modeling Of Coal Pillars In Steeply Inclined Coal Seams - Case Study: Hamkar Coal Mine. Journal Of Analytical And Numerical Methods In Mining Engineering, 6(11), 27-38. (In Persian).
- [15] Dehghan, S., Shahriar, K., Maarefvand, P., Goshtasbi, K. (2012). Estimation of Applied Stresses on Pillars in Stope and Rib Pillar mining Method by Numerical and Empirical Methods in Fetr 6 Chromite Mine. Journal of Analytical and Numerical Methods in Mining Engineering, 2(3), 53-61.
- [16] Aydan, Ö. & Kawamoto, T. (2004). "The damage to abandoned lignite mines caused by the 2003 Miyagi-Hokubu earthquake and some considerations on its causes". 3rd Asian Rock Mechanics Symposium, Kyoto, 525-530. (2004).
- [17] Nishida, N., Esaki, T., Aoki, K. and Kameda, K. (1984) "Evaluation and prediction of subsidence in old working areas and practical and preventive measures against mining damage to new structures. Proceedings of Third International Symposium on Land Subsidence", Venice.
- [18] Aydan, Ö., Ohta, Y., Geniş, M., Tokashiki, N., & Ohkubo, K. (2010). Response and stability of underground structures in rock mass during earthquakes. Rock mechanics and rock engineering, 43(6), 857-875.
- [19] Tabas Coal Mine. Rock Mechanics Reports. Thecnical Office (2014).
- [20] Itasca, 2005. FLAC3D-Fast Lagrangian Analysis of Continua-User Manuel (dynamic option) (Version 2.1).